Photoassociative Production and Trapping of Ultracold KRb Molecules

D. Wang,[1] J. Qi,[1] M. F. Stone,[1] O. Nikolayeva,[2] H. Wang,[3] B. Hattaway,[1] S. D. Gensemer,[4] P. L. Gould,[1] E. E. Eyler,[1] and W. C. Stwalley[1]

[1]*Physics Department, University of Connecticut, Storrs, Connecticut 06269, USA*
[2]*Physics Department, University of Latvia, 19 Rainis Boulevard, Riga, Latvia 15986*
[3]*The Aerospace Corporation, M2-253, 2350 East El Segundo Boulevard, El Segundo, California 90245-4691, USA*
[4]*Van der Waals-Zeeman Institut, Universiteit van Amsterdam, Valckenierstraat 65, 1018 XE Amsterdam, The Netherlands*

(Received 16 July 2004; published 7 December 2004)

We have produced ultracold heteronuclear KRb molecules by the process of photoassociation in a two-species magneto-optical trap. Following decay of the photoassociated KRb*, the molecules are detected using two-photon ionization and time-of-flight mass spectroscopy of KRb^+. A portion of the metastable triplet molecules thus formed are magnetically trapped. Photoassociative spectra down to 91 cm^{-1} below the $K(4s) + Rb(5p_{1/2})$ asymptote have been obtained. We have made assignments to all eight of the attractive Hund's case (c) KRb* potential curves in this spectral region.

DOI: 10.1103/PhysRevLett.93.243005 PACS numbers: 33.80.Ps, 32.80.Pj, 33.20.–t, 34.50.Gb

The study of ultracold molecules has seen rapid progress in recent years [1]. Homonuclear molecules have been produced at ultracold temperatures, here defined as $T < 1$ mK, by photoassociating ultracold atoms [2,3]. In a few cases, the resulting molecules have been subsequently trapped [4,5]. Feshbach resonances in even colder atomic samples have yielded very weakly bound homonuclear molecules [6], in some cases under quantum degenerate conditions. Heteronuclear polar molecules have attracted particular interest because their permanent dipole moments can be controlled with external fields. At ultracold temperatures, the resulting long-range, anisotropic dipole-dipole interactions are expected to lead to new phenomena, such as anisotropic collisions [7] and novel quantum degenerate behavior [8–10]. Heteronuclear photoassociative spectroscopy [11] is also of interest, and applications of ultracold polar molecules to quantum computing [12] and fundamental symmetries [13] are also being considered.

We report here on the production, detection, magnetic trapping, and photoassociation spectroscopy of KRb molecules. This work builds on a variety of other recent advances, particularly the recent production and spectroscopic study of ultracold polar RbCs molecules by Kerman and co-workers [14,15], using photoassociation (PA) in overlapping Rb and Cs magneto-optical traps (MOTs). Similar PA spectroscopy has been performed with the heteronuclear (but nonpolar) $^6Li^7Li$ molecule [16]. Observations of ultracold $NaCs^+$ and NaCs [17], RbCs [18], and KRb [19] have been reported in two-species MOTs, although the formation mechanisms have not been identified. Heteronuclear Feshbach resonances have been recently reported in Li + Na [20] and K + Rb [21], although the resulting molecules were not directly observed. At temperatures above 10 mK, polar molecules have been successfully cooled and trapped. CaH has been buffer-gas cooled and magnetically trapped [22], while ND_3 has been electrostatically slowed and loaded into electric traps [23,24].

Photoassociation, as shown in Fig. 1, involves the free-bound absorption of a photon by a colliding pair of atoms [2,3]. It is a particularly powerful spectroscopic technique at μK temperatures, where only partial waves with $\ell \lesssim 3$ can contribute, restricting molecule formation to the lowest rotational levels, $J \lesssim 4$.

In our experiments, electronically excited KRb* molecules are produced by PA in overlapping K and Rb MOTs, followed by radiative stabilization via decay to the ground $X^1\Sigma^+$ state or the metastable $a^3\Sigma^+$ state. Dark-spot MOTs are used to achieve high atomic densities, and ionization detection is employed for improved sensitivity. We observe trapping of ultracold heteronuclear molecules for the first time, by confining triplet KRb molecules in the inhomogeneous magnetic field of the MOT. We also present high-resolution photoassociative spectra down to 91 cm^{-1} below the $K(4s) + Rb(5p_{1/2})$ asymptote. In these spectra we have identified transitions to all eight of the attractive long-range potentials converging to $4s + 5p_{1/2}$ and $4s + 5p_{3/2}$.

Our $^{39}K/^{85}Rb$ dual species MOT uses the same apparatus previously used for trapping ^{39}K [25] with the addition of trap and repump beams for ^{85}Rb. Frequently the K and Rb diode laser beams can share optics, because of the closeness of the resonance energies (see Fig. 1). Indeed it is this near degeneracy which makes the KRb C_6 values especially large [11]. Normally we operate both atom traps as "dark-spot" MOTs [26], with typical densities of $10^{11}/cm^3$ for Rb and $3 \times 10^{10}/cm^3$ for K.

To achieve sensitive and species-selective detection we employ two-photon ionization at 602.5 nm followed by time-of-flight mass spectroscopy, as shown in the inset of Fig. 2. The ionizing laser pulse

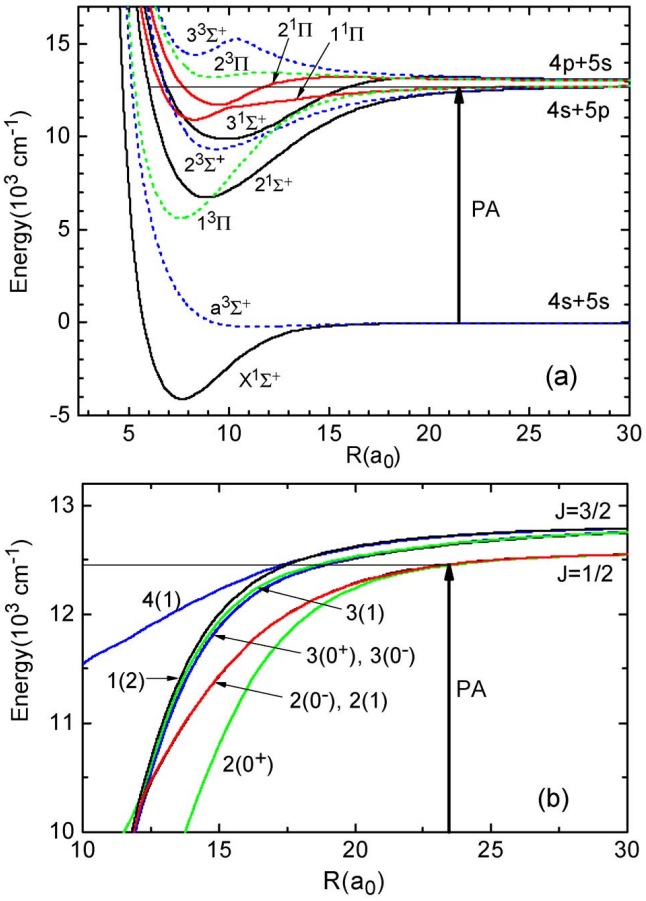

FIG. 1 (color online). The photoassociation process (PA) in KRb based on the *ab initio* potential energy curves of Ref. [28]. Subsequent to PA, radiative decay populates the $X^1\Sigma^+$ or $a^3\Sigma^+$ states. In (b), the long-range states converging to $4s + 5p_J$ are shown; the state designations consist of an ordinal numbering followed by the Hund's case (c) symmetry in parentheses, expressed as $\Omega^{\pm}$. The long-range states converging to $4p_J + 5s_{1/2}$ (not shown) are all repulsive.

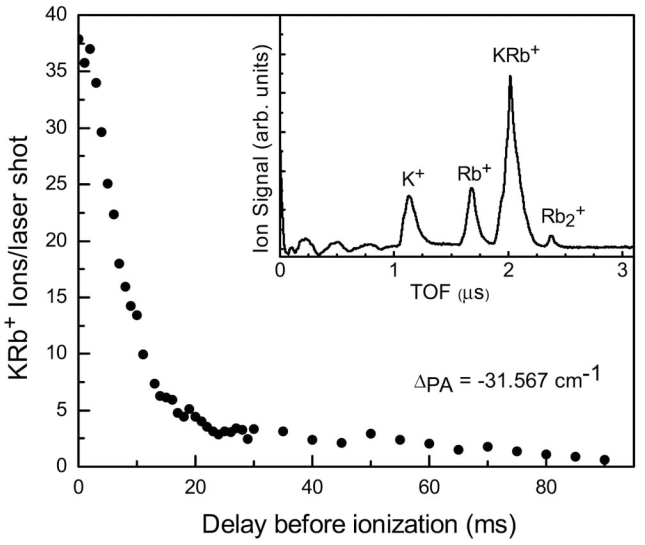

FIG. 2. Main panel: Time evolution of the $^{39}K^{85}Rb^+$ signal as a function of the delay of the ionization pulse relative to the turnoff of the PA laser, with the PA laser set to a $3(0^-)$ state resonance as indicated in Fig. 3(a). PA laser detuning Δ_{PA} is measured relative to $K(4s, F = 1) + Rb(5p_{1/2}, F = 2)$. Inset: Typical time-of-flight mass spectrum, with the PA laser tuned to the same resonance.

(1.5 mJ, ~10 ns) is focused to provide a typical peak intensity of 7×10^6 W/cm^2. These pulses are generated using a doubled Nd:YAG laser at 532 nm to pump a pulsed dye laser at 10 Hz. Ion signals can also be obtained using a 532 nm laser directly. A Channeltron is used to detect atomic and molecular ions. We obtain PA spectra by tuning a cw tunable PA laser (Coherent 899-29, typically >400 mW) while detecting the KRb^+ signal.

We obtain typical signals of 10–60 KRb^+ ions per laser shot when the PA laser is tuned to a strong KRb resonance. Surprisingly, these signals are comparable to the Rb_2^+ ion signals observed when photoassociating on a strong Rb_2 line. The number of colliding atom pairs available at the Condon radius, where the PA laser matches the ground-excited free-bound transition, strongly favors Rb_2. Its resonant-dipole $1/R^3$ potentials permit photoassociation at much longer range (e.g., 100 a_0) compared to KRb where the van der Waals $1/R^6$ potential results in shorter-range excitation (e.g., 30 a_0). However, the Franck-Condon factors for decay to the $1/R^6$ ground-state potentials strongly favor KRb. Therefore we expect to produce less KRb* in the PA step, but with more efficient decay to a bound state. This is reflected in the barely detectable KRb trap loss signal we observe in contrast to losses of 10–50% for Rb_2. Also, the relaxed heteronuclear selection rules allow more PA pathways in KRb compared to Rb_2 [11]. The signal sizes may also be influenced by different detection efficiencies for the KRb and Rb_2. Finally, the signal sizes may be enhanced by magnetic trapping, discussed below. Ignoring this trapping and assuming 100% ionization efficiency for KRb and 50% ion detection efficiency, our maximum signal size would correspond to a production rate of about 4×10^4 KRb molecules/s.

We observe trapping of triplet KRb molecules in the magnetic field of the MOT coils [5]. These molecules must be in the triplet a state since the singlet molecules have zero magnetic moment. We can investigate the trapping by turning off the PA laser while leaving the MOT lasers and magnetic field on, then firing the detection laser pulse after a variable delay time. Figure 2 shows a decay curve observed as a function of this delay, with the laser tuned to a strong KRb resonance [the $3(0^-)$ transition in Fig. 3(a)]. The background of 1.7 ions/shot due to KRb formed in the absence of the PA laser [19] has been subtracted from this decay curve. A significant fraction

of the molecules survive long past the ballistic decay time, which is about 3 ms for our 1 mm diameter detection beam, assuming a temperature of $\sim 300\ \mu$K. The trapped molecules appear to decay nonexponentially, with a small signal still observable after 150 ms. Because the atoms in the MOT are unpolarized, we expect the molecules to have a wide distribution of projection quantum numbers (m_J or m_F, depending on the coupling scheme), giving rise to a large spread in the effective trapping potential. For a molecule with the largest possible magnetic dipole moment projection of two Bohr magnetons ($2\mu_B = q_e\hbar/m_e$), the horizontal trapping potential reaches a depth of 500 μK with a radius of 2.5 mm. The vertical potential is slightly distorted by gravity, but the magnetic trapping force is 2.5 times larger than the gravitational force. Molecules with smaller magnetic dipole moment projections will experience weaker trapping, and can be expected to be confined in a larger trap volume, with a higher escape rate and lower detection efficiency. At least 2/3 of the total molecules formed will be untrapped or antitrapped.

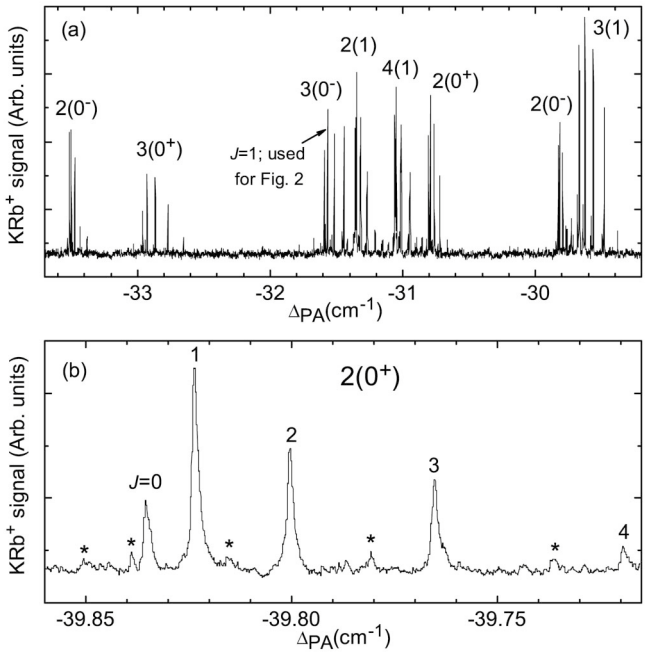

FIG. 3. (a) A PA spectrum for $^{39}K^{85}Rb$ showing eight vibrational bands as our PA laser is scanned as indicated below the K(4s) + Rb(5$p_{1/2}$) asymptote. The rotational spacings vary widely, with smaller spacings corresponding to longer-range states. This spectrum includes transitions to seven of the eight states correlating with the $J = 1/2$ and $J = 3/2$ asymptotes. All these states can be reached by dipole-allowed transitions from colliding ground-state atoms ($\Omega = 0^{\pm}, 1$). (b) A high-resolution PA spectrum showing the rotational structure as the PA laser detuning is scanned through a $2(0^+)$ state resonance. The asterisks (*) indicate "hyperfine ghosts" due to a small population in the "bright" $F = 2$ state of $K(4s)$ in our dark-spot MOT.

Examples of our heteronuclear PA spectra are given in Fig. 3. The observed linewidths vary from about 35–500 MHz, primarily due to unresolved internal structure. The excellent signal-to-noise ratio makes the spectra readily assignable. At these low J values, rotational series such as the one shown in Fig. 3(b) are fit precisely by a linear plot of energy versus $[J(J+1) - \Omega^2]$, yielding a rotational constant B_v without observable centrifugal distortion. The four $0^{\pm}$ states (two of each), the three $\Omega = 1$ states, and the sole $\Omega = 2$ state are readily assigned in this way. Our $\pm$ assignments are preliminary because of extensive perturbations [27]. These effects are evident in Fig. 4, which plots the vibrational energies and B_v values for one of the 0^+ states. We make nominal assignments by associating the state having the smaller C_6 coefficient with the shorter outer turning point and therefore the larger rotational constant. Thus the series in Fig. 4 is assigned to the $2(0^+)$ state at the K(4s) + Rb(5$p_{1/2}$) asymptote, shown in Fig. 1(b). Figure 3(b) in particular corresponds to the ninth observed vibrational level in the Fig. 4 series. There are eight vibrational levels in Fig. 3(a), assigned as 0 or 1 states depending on their lowest rotational quantum number ($J = 0$ or 1). One of the 0 levels corresponds to the 11th level in the $2(0^+)$ series in Fig. 4. Two other 0 levels must correspond to $2(0^-)$, with a vibrational spacing comparable to $2(0^+)$ at this detuning. The final two 0 levels, with larger vibrational spacings, are assigned to the $3(0^-)$ and $3(0^+)$ states, respectively, in order of increasing B_v.

In a similar way, among the three $\Omega = 1$ levels, one fits well in a long vibrational series, similar to the $2(0^+)$ series in Fig. 4, and is assigned to the 2(1) state. The other two levels cannot be in the 2(1) series and are assigned to the 3(1) and the 4(1) states based on their relative rotational constants. Since four vibrational levels of the 1(2) state have also been observed at other detun-

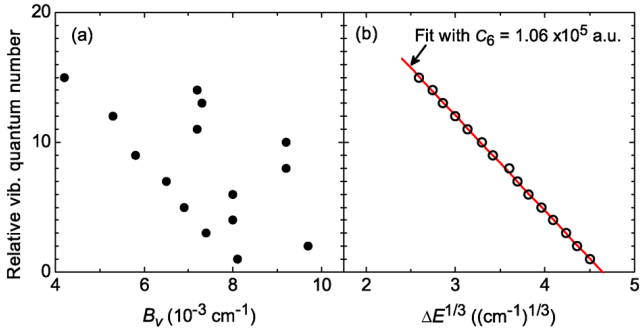

FIG. 4 (color online). (a) The rotational constants B_v in cm^{-1} and (b) the detuning (binding energy) to the 1/3 power for levels of the $2(0^+)$ states converging to the K(4s) + Rb(5$p_{1/2}$) asymptote versus relative vibrational quantum number (absolute values unknown). For a pure R^{-6} long-range potential, these plots should be linear in the absence of perturbations [33,34].

ings, we have been able to observe all eight of the Hund's case (c) electronic states correlating to the $K(4s) + \mathrm{Rb}(5p_{1/2,3/2})$ asymptotes, as shown in Fig. 1(b). Further discussion of these assignments will be published elsewhere [27].

Because of our ion extraction configuration, the molecules are formed in a dc field of ~ 160 V/cm. We observe no Stark effect at our spectral resolution of ~ 0.001 cm^{-1}, consistent with the small dipole moment ($< 0.04\ ea_0$) predicted for KRb* [28–31]. This differs from the RbCs case of Ref. [14], where both the field (390 V/cm) and the dipole moment ($\sim 0.5\ ea_0$) are larger. We note that the dipole moments of the $X^1\Sigma^+$ and $a^3\Sigma^+$ states of KRb at their equilibrium separations are $-0.30(2)$ and $-0.02(1)$ ea_0, respectively [32].

Assuming our assignments are correct for the $2(0^+)$, $2(0^-)$, and 2(1) states, one can estimate the corresponding effective C_6 values [33,34] as $(1.06 \pm 0.06) \times 10^5$, $(1.01 \pm 0.04) \times 10^5$, and $(1.01 \pm 0.05) \times 10^5$ atomic units (a.u.), respectively. Note that C_6 is a weak function of R between very long-range (spin-orbit $\gg$ dispersion) and intermediate range (dispersion $\gg$ spin-orbit)—the calculations of [35], for example, vary from 1.0×10^5 a.u. at very long range to 3.1×10^5 a.u. at intermediate range for the $2(0^+)$ state. Model calculations to better define the dispersion interaction are under way.

It is important to consider the effects of symmetry on molecule formation. Some relevant transition dipole moment functions are available [32]. For levels near dissociation, all of the excited states we produce decay with $\gtrsim 75\%$ probability to the $a^3\Sigma^+$ state. In fact, the $2(0^-)$, $2(0^-)$, and 1(2) states radiate 100% to this triplet state. Thus, since we observe KRb^+ from 0^- and 2 states, we know our ion detection is sensitive to triplet molecules. However, since even the 0^+ and 1 states radiate primarily to triplet states at long range, we do not yet know if our ionization detection is sensitive to singlet molecules. We hope that in future experiments where both singlet and triplet molecules are produced but only triplets are trapped, we can determine the relative sensitivity for singlet and triplet molecule detection.

In summary, we have significantly advanced the study of ultracold polar molecules, trapping them for the first time. KRb molecules are produced by photoassociation and detected by ionization. We have extensively explored the PA spectrum, identifying all eight of the electronic states expected near the $K(4s) + Rb(5p)$ limits.

We gratefully acknowledge support from the National Science Foundation and the University of Connecticut Research Foundation, helpful discussions with Warren Zemke, Tom Bergeman, David DeMille and Jamie Kerman, and laboratory assistance from Andrew Scott and Ye Huang.

[1] J. T. Bahns, P. L. Gould, and W. C. Stwalley, Adv. At. Mol. Opt. Phys. **42**, 171 (2000).
[2] W. C. Stwalley and H. Wang, J. Mol. Spectrosc. **195**, 194 (1999).
[3] F. Masnou-Seeuws and P. Pillet, Adv. At. Mol. Opt. Phys. **47**, 53 (2001).
[4] T. Takekoshi, B. M. Patterson, and R. J. Knize, Phys. Rev. Lett. **81**, 5105 (1998).
[5] N. Vanhaecke *et al.*, Phys. Rev. Lett. **89**, 063001 (2002).
[6] K. E. Strecker, G. B. Partridge, and R. G. Hulet, Phys. Rev. Lett. **91**, 080406 (2003); M. Greiner, C. A. Regal, and D. S. Jin, Nature (London) **426**, 537 (2003); J. Cubizolles *et al.*, Phys. Rev. Lett. **91**, 240401 (2003); M. W. Zwierlein *et al.*, Phys. Rev. Lett. **91**, 250401 (2003); S. Jochim *et al.*, Science **302**, 2101 (2003); S. Dürr *et al.*, Phys. Rev. Lett. **92**, 020406 (2004).
[7] J. L. Bohn, Phys. Rev. A **63**, 052714 (2001).
[8] L. Santos *et al.*, Phys. Rev. Lett. **85**, 1791 (2000).
[9] S. Yi and L. You, Phys. Rev. A **61**, 041604(R) (2000).
[10] K. Goral, L. Santos, and M. Lewenstein, Phys. Rev. Lett. **88**, 170406 (2002).
[11] H. Wang and W. C. Stwalley, J. Chem. Phys. **108**, 5767 (1998).
[12] D. DeMille, Phys. Rev. Lett. **88**, 067901 (2002).
[13] M. G. Kozlov and L. N. Labzowsky, J. Phys. B **28**, 1933 (1995).
[14] A. J. Kerman *et al.*, Phys. Rev. Lett. **92**, 033004 (2004).
[15] A. J. Kerman *et al.*, Phys. Rev. Lett. **92**, 153001 (2004).
[16] U. Schlöder, C. Silber, and C. Zimmermann, Appl. Phys. B **73**, 801 (2001).
[17] J. P. Shaffer, W. Chalupczak, and N. P. Bigelow, Phys. Rev. Lett. **82**, 1124 (1999); C. Haimberger *et al.*, Phys. Rev. A **70**, 021402(R) (2004).
[18] H. Wang, Bull. Am. Phys. Soc. **48**, J1.025 (2003).
[19] M. W. Mancini *et al.*, Phys. Rev. Lett. **92**, 133203 (2004).
[20] C. A. Stan *et al.*, Phys. Rev. Lett. **93**, 143001 (2004).
[21] S. Inouye *et al.*, Phys. Rev. Lett. **93**, 183201 (2004).
[22] J. D. Weinstein *et al.*, Nature (London) **395**, 148 (1998).
[23] H. L. Bethlem *et al.*, Nature (London) **406**, 491 (2000).
[24] F. M. H. Crompvoets *et al.*, Nature (London) **411**, 174 (2001).
[25] H. Wang, P. L. Gould, and W. C. Stwalley, Phys. Rev. A **53**, R1216(R) (1996).
[26] W. Ketterle *et al.*, Phys. Rev. Lett. **70**, 2253 (1993).
[27] D. Wang *et al.*, Eur. Phys. J. D (to be published).
[28] S. Rousseau *et al.*, J. Mol. Spectrosc. **203**, 235 (2000).
[29] S. J. Park *et al.*, Chem. Phys. **257**, 135 (2003).
[30] S. Kotochigova (private communication).
[31] W. T. Zemke and W. C. Stwalley, J. Chem. Phys. **120**, 88 (2004).
[32] S. Kotochigova, P. S. Julienne, and E. Tiesinga, Phys. Rev. A **68**, 022501 (2003).
[33] R. J. Le Roy, in *Molecular Spectroscopy 1*, edited by R. F. Barrow *et al.* (Chem. Soc. London, London, 1973), p. 113.
[34] W. C. Stwalley, Contemp. Phys. **19**, 65 (1978).
[35] B. Bussery, Y. Achkar, and M. Aubert-Frecon, Chem. Phys. **116**, 319 (1987).